

UC Davis

UC Davis Previously Published Works

Title

Structural mechanisms underlying activation of TRPV1 channels by pungent compounds in gingers

Permalink

<https://escholarship.org/uc/item/6043x3qn>

Journal

British Journal of Pharmacology, 176(17)

ISSN

0007-1188

Authors

Yin, Yue
Dong, Yawen
Vu, Simon
[et al.](#)

Publication Date

2019-09-01



DOI

10.1111/bph.14766

Peer reviewed

RESEARCH PAPER

Structural mechanisms underlying activation of TRPV1 channels by pungent compounds in gingers

Yue Yin¹ | Yawen Dong¹ | Simon Vu² | Fan Yang³ | Vladimir Yarov-Yarovoy² |
Yuhua Tian¹  | Jie Zheng² 

¹Department of Pharmacology, Qingdao University School of Pharmacy, Qingdao, Shandong, China

²Department of Physiology and Membrane Biology, UC Davis School of Medicine, Davis, CA, USA

³Department of Biophysics and Kidney Disease Center, First Affiliated Hospital, Institute of Neuroscience, National Health Commission and Chinese Academy of Medical Sciences Key Laboratory of Medical Neurobiology, Zhejiang University School of Medicine, Hangzhou, Zhejiang, China

Correspondence

Yuhua Tian, Department of Pharmacology, Qingdao University School of Pharmacy, Qingdao, Shandong, China.
Email: yhtian05250@qdu.edu.cn

Jie Zheng, Department of Physiology and Membrane Biology, UC Davis School of Medicine, Davis, CA 95616, USA.
Email: jzheng@ucdavis.edu

Funding information

National Institute of Neurological Disorders and Stroke, Grant/Award Number: R01NS103954; Qingdao Postdoctoral Research Project, Grant/Award Number: R01NS103954

Background and Purpose: Like chili peppers, gingers produce pungent stimuli by a group of vanilloid compounds that activate the nociceptive transient receptor potential vanilloid 1 (TRPV1) ion channel. How these compounds interact with TRPV1 remains unclear.

Experimental Approach: We used computational structural modelling, functional tests (electrophysiology and calcium imaging), and mutagenesis to investigate the structural mechanisms underlying ligand–channel interactions.

Key Results: The potency of three principal pungent compounds from ginger – shogaol, gingerol, and zingerone—depends on the same two residues in the TRPV1 channel that form a hydrogen bond with the chili pepper pungent compound, capsaicin. Computational modelling revealed binding poses of these ginger compounds similar to those of capsaicin, including a “head-down tail-up” orientation, two specific hydrogen bonds, and important contributions of van der Waals interactions by the aliphatic tail. Our study also identified a novel horizontal binding pose of zingerone that allows it to directly interact with the channel pore when bound inside the ligand-binding pocket. These observations offer a molecular level explanation for how unique structures in the ginger compounds affect their channel activation potency.

Conclusions and Implications: Mechanistic insights into the interactions of ginger compounds and the TRPV1 cation channel should help guide drug discovery efforts to modulate nociception.

1 | INTRODUCTION

Spiciness is a type of chemosensation elicited by certain plant products and transmitted by the somatosensation pathway instead of the taste (gustation) pathway. Cloning of the TRPV1 cation channel (Caterina et al., 1997), the receptor for pungent chili pepper compound capsaicin, marks the beginning of a new era of mechanistic investigation into sensory physiology for spiciness. TRPV1 channels are non-selective cation channels sensitive to diverse physical and chemical stimuli including heat, low extracellular pH, animal toxins,

and many spicy molecules (Caterina et al., 1997; Han et al., 2018; Siemens et al., 2006; Tominaga et al., 1998; Yang, Yang, et al., 2015; Zheng, 2013). As a polymodal nociceptor, the TRPV1 channel offers ample opportunities to gain insight into basic sensory physiology and to treat pain via pharmaceutical manipulation. Important recent breakthroughs have been made in understanding how TRPV1 channels are activated by capsaicin (Yang & Zheng, 2017). How other spicy compounds are sensed by the TRPV1 channel is however less understood.

Capsaicin activation of TRPV1 channels represents an impressive case of ligand–host interaction. Solving high-resolution cryo-electron microscopy (cryo-EM) structures of TRPV1 channels in their apo and capsaicin-bound states was a major breakthrough in understanding capsaicin-induced spiciness (Cao, Liao, Cheng, & Julius, 2013; Liao,

Abbreviations: cryo-EM, cryo-electron microscopy; mTRPV1, mouse TRPV1 cation channel; rTRPV1, rat TRPV1 cation channel; VDW, van der Waals; WT, wild type

Yue Yin, Yawen Dong, and Simon Vu have equal contribution.

Cao, Julius, & Cheng, 2013). Based on these structures, the atomic interactions between capsaicin and the TRPV1 channel were deduced by a combination of computational structural modelling and functional methods and by molecular dynamic simulations (Darre & Domene, 2015; Elokely et al., 2016; Yang, Xiao, et al., 2015; Figure 1a). Key atomic interactions include two hydrogen bonds—formed between the amide group in the capsaicin neck and the hydroxyl group of T551 on the S4 segment of the TRPV1 channel (using mTRPV1 amino acid number) and between the hydroxyl group in the capsaicin head and the carboxyl group of E571 on the S4-S5 linker—as well as extensive van der Waals (VDW) interactions including those by the capsaicin tail. Accuracy of the current capsaicin binding model has been satisfactorily confirmed by studies of the structural correlates of deactivation kinetics (Kumar et al., 2016), the activation conformational wave in TRPV1 channels triggered by capsaicin binding (Yang et al., 2018), the evolutionary drive for the tree shrew's insensitivity to spiciness (Han et al., 2018), and the rational designs of vanilloid-sensitive TRPV2 channel mutants (Yang, Vu, Yarov-Yarovoy, & Zheng, 2016; Zhang et al., 2016).

Gingers (*Zingiber officinale* Roscoe) are fresh or dried rhizomes of the family Zingiberaceae. They are old-world food condiments that are pungent, like the chili peppers which originated in the Americas, though less powerful in imparting heat to a food dish. Gingers introduce a rich and dynamic dimension to food flavour that can be manipulated by cooking methods. They have been used in culinary and medicinal practices for over 2,000 years. The westward voyages of Christopher Columbus—which led to the discovery of chili peppers in the Americas—were partially motivated by the goal of finding a shorter route for shipping spices such as gingers from Asia (Parry, 1969). Ginger products are also used in the treatment of various diseases such as gastric ulcer, pain, and cancer (Chrubasik, Pittler, & Roufogalis, 2005; Grant & Lutz, 2000). Taking ginger extract pills or candies is a popular practice believed to prevent seasickness (Aslani, Ghannadi, & Rostami, 2016; Lien et al., 2003). It is therefore not surprising that there has been a long and fruitful history of investigation into the active components of ginger and their properties (Govindarajan, 1982a, 1982b). Ginger compounds were carefully examined both before and after the discovery of TRPV1 channels (Dedov et al., 2002; Govindarajan, 1982a), with their binding mode in the TRPV1 channel proposed even before high-resolution channel structures were known (Ohbuchi et al., 2016). In light of the recently revealed cryo-EM structures of the TRPV1 channel and details of capsaicin-TRPV1 channel interactions, the opportunity to solve the nature of ginger compounds binding has arisen.

Gingers produce many pungent compounds that are members of the shogaol, gingerol, and zingerone families (Figure 1b). These compounds share certain structural features with capsaicin. In particular, they contain the same vanillyl head group, with structural differences being found in both the neck and tail regions. It is known that ginger compounds can directly activate TRPV1 channels, though they are less potent than capsaicin (Dedov et al., 2002; Iwasaki et al., 2006; Kobata et al., 2006). While previous studies have illustrated many pharmacological properties associated with activation of TRPV1 channels by

What is already known

- Ginger compounds target the nociceptive TRPV1 ion channel to produce their pungency.

What this study adds

- We report the structural mechanisms underlying ginger compound-TRPV1 complex formations.
- Similarities and differences between capsaicin and ginger compounds in their interactions with TRPV1 were identified.

What is the clinical significance

- Findings from this study should help drug discovery efforts to regulate nociceptive function.

ginger compounds, the structural mechanism underlying the ligand-TRPV1 channel interaction is unclear.

In the present study, we combined calcium imaging, electrophysiology, mutagenesis, and computational structural modelling to explore the molecular nature of TRPV1 channel activation by three representative pungent ginger compounds: **6-shogaol**, **6-gingerol**, and zingerone. Our results demonstrated that these compounds bind to TRPV1 channels in a manner similar to that of capsaicin, including the “head-down tail-up” orientation and the key contributions of two hydrogen bonds and VDW interactions from the tail. Distinct structural features, especially those in the tail, cause large differences in potency and can even alter the manner of ligand-channel interaction. The correlation between structural features in capsaicin and ginger compounds and their pungency derived from the present study should benefit pharmaceutical efforts seeking for novel analgesics.

2 | METHODS

2.1 | cDNAs

Murine TRPV1 channels (a gift from Dr. Michael X. Zhu, University of Texas Health Science Center at Houston) was used in the present study. Enhanced yellow fluorescent protein was fused to the C terminus of the TRPV1 channel to help identify channel-expressing cells. Tagging of enhanced yellow fluorescent protein did not change the functional properties of TRPV1 channels, as reported previously (Cheng, Yang, Takahashi, & Zheng, 2007). Point mutations of mTRPV1 were generated by overlapping PCR and confirmed by sequencing (Yang, Xiao, et al., 2015).

2.2 | Cell culture and transfection

HEK293 cells were cultured in DMEM supplemented with 10% FBS, penicillin (100 U·ml⁻¹), and streptomycin (100 mg·ml⁻¹) for 24 to

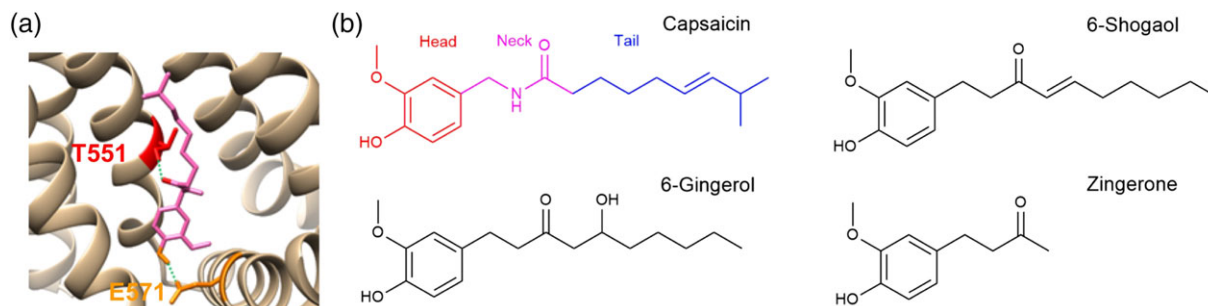


FIGURE 1 Comparison of the pungent compounds from chili pepper and ginger. (a) A zoomed-in view of the capsaicin-binding pocket demonstrating the structural model of capsaicin-TRPV1 channel interactions. The capsaicin molecule is shown in pink, with the hydrogen bond-forming groups in the neck and head shown in red and orange, respectively. The TRPV1 channel is shown in beige, with the two residues making hydrogen bonds with capsaicin, T551 and E571, highlighted in red and orange, respectively. (b) Chemical structures of capsaicin, 6-shogaol, 6-gingerol, and zingerone. All four compounds possess a vanillyl moiety and are structurally similar, with the differences being in the neck and tail regions

48 hr at 37°C to reach 50% to 70% confluency. Transient transfection mediated by lipofectamine 2000 was conducted following the manufacturer's protocol. Calcium imaging and patch-clamp recording were done 24 hr after transfection.

2.3 | Live-cell Ca^{2+} imaging assay

Transfected HEK293 cells were incubated with Fluo-4 AM in the Ca^{2+} imaging solution (140-mM NaCl, 5-mM KCl, 1-mM MgCl_2 , 1.8-mM CaCl_2 , 10-mM glucose, and 15-mM HEPES, pH 7.4) in the dark at room temperature for 50 min. Incubated cells were washed twice with the Ca^{2+} imaging solution before recording. An Olympus IX73 microscope equipped with an Olympus DP80 CCD camera was used for fluorescence imaging. A blue filter (460 to 495 nm) and a long-pass filter (510 nm) were used as the excitation and emission filters, respectively, in conjunction with a dichroic mirror at 505 nm. Grey-scale fluorescence intensity of individual cells was collected and quantified using the Nikon confocal image analysis software (NIS Elements AR Analysis). Stimulation of the TRPV1 channels with different concentrations of agonists was achieved by perfusion with a rapid solution change system (RSC-200, Bio-Logic Science Instruments); capsaicin (10 μM) was used as a positive control for normalization of the fluorescence intensity levels.

2.4 | Electrophysiology

Patch-clamp recordings were done in the inside-out configuration using an EPC10 amplifier driven by PatchMaster software (both from HEKA). Cell membrane potential was held at 0 mV, from which the voltage was first stepped to +80 mV for 300 ms and then to -80 mV for 300 ms. Currents were recorded and presented at both +80 mV and -80 mV; statistical analyses were done with currents measured at +80 mV. Both the pipette solution and bath solution contained 130-mM NaCl, 3-mM HEPES, and 0.2-mM EDTA, pH 7.2. Current signals were filtered at 2.5 kHz and sampled at 10 kHz. Macroscopic current amplitude was determined after subtracting off the

leakage current and normalized to the maximal current response to 10- μM capsaicin. Single-channel amplitudes of wild-type (WT) and mutant channels were measured at several agonist concentrations.

2.5 | Data and statistical analysis

The data and statistical analysis in this study comply with the recommendations of the *British Journal of Pharmacology* on experimental design and analysis in pharmacology (Curtis et al., 2018). Cells were randomly selected for live-cell calcium imaging analysis or patch recording. Data analysis for experiments presented was performed in a blinded manner. Functional differences caused by changes in agonists or point mutations were tested using one-way ANOVA followed by Tukey's post hoc test or Student's *t* tests when appropriate; $P < .05$ was considered statistically significant. Post hoc tests have been performed when ANOVA analysis indicated that a significant difference existed between the groups. Individual agonist concentration dependence of fluorescence intensity or current amplitude was fitted to a Hill equation to obtain estimates of the EC_{50} and slope factor values. Estimates from multiple measurements were subjected to statistical analyses for potential differences; their mean \pm SEM values (together with the *n* number) are reported. For illustrations, averaged agonist concentration dependence of fluorescence intensity or current amplitude was plotted and fitted to a Hill equation. Single-channel recordings were analysed by building an all-point histogram, which was fitted to a sum of Gaussian functions using the IGOR PRO software (WaveMetrics). The position of Gaussian peaks represented the average current amplitude, and the fractional area under the peaks represented the percentage of time the channel dwelled in the closed and open states.

2.6 | Computational structural modelling

Docking of the vanilloid compounds was performed using the RosettaLigand application within the Rosetta molecular modelling software suite, version 3.7 (Bender et al., 2016; Davis & Baker, 2009; Davis, Raha, Head, & Baker, 2009; Meiler & Baker, 2006), in an XML

style script in RosettaScripts (Lemmon & Meiler, 2012). The rTRPV1 capsaicin-bound cryo-EM structure (PDB ID: 3J5R) was first relaxed in a membrane environment using RosettaMembrane (Barth, Schonbrun, & Baker, 2007; Yarov-Yarovoy et al., 2012; Yarov-Yarovoy, Baker, & Catterall, 2006; Yarov-Yarovoy, Schonbrun, & Baker, 2006). Vanilloid compounds were initially placed at the centre of the binding pocket within the S3, S4, S4-S5 linker, and S6 segments, and were constrained within a 10-Å diameter sphere where it was allowed to move freely. A total of 200 conformers for each compound were generated using Open Eye OMEGA software (Hawkins & Nicholls, 2012; Hawkins, Skillman, Warren, Ellingson, & Stahl, 2010). A total of 30,000 ligand-channel complex models were generated. To determine the best model, they were first screened for total energy. The 3,000 lowest energy models were then further screened for binding energy between the compound and the channel. The top 30 models were identified as candidates. All molecular graphics were rendered by UCSF Chimera software version 1.13 (Pettersen et al., 2004).

To quantify the docking results for structural convergence, the binding energy value for the 3,000 lowest energy models was plotted against its un-superimposed ligand root mean squared deviation. The lowest binding energy model was used as a reference.

To define potential atomic interactions, binding energy was determined to be mainly hydrogen bond and VDW energies (calculated by the sum of attractive and repulsive energies). These interactions were further mapped on a per residue basis using Rosetta's residue_energy_breakdown function.

2.7 | Materials

Capsaicin was obtained from Abcam (Cambridge, UK). 6-Shogaol and zingerone were obtained from Chengdu Biopurify Phytochemicals Ltd (China). Capsazepine and 6-gingerol were obtained from MedChemExpress (USA). The purity of these compounds is above

98%. Fluo-4 AM and lipofectamine 2000 were obtained from Thermo Fisher Scientific (Waltham, MA, USA).

2.8 | Nomenclature of targets and ligands

Key protein targets and ligands in this article are hyperlinked to corresponding entries in <http://www.guidetopharmacology.org>, the common portal for data from the IUPHAR/BPS Guide to PHARMACOLOGY (Harding et al., 2018), and are permanently archived in the Concise Guide to PHARMACOLOGY 2017/18 (Alexander et al., 2017).

3 | RESULTS

3.1 | Activation of mTRPV1 channels by ginger compounds

Gingers contain a number of spicy vanilloid compounds that are known to directly activate human and rat TRPV1 channels (Dedov et al., 2002; Iwasaki et al., 2006). In order to investigate the structural mechanism underlying their ligand-host interactions, we first tested representative ginger compounds on mouse TRPV1 channels, from which specific capsaicin-channel interactions had been previously derived (Yang, Xiao, et al., 2015). Patch-clamp recordings revealed concentration-dependent activation of mTRPV1 channels by each of the three compounds (Figure 2a; Table 2), among which 6-shogaol was the most potent, with an EC_{50} value of $1.4 \pm 0.1 \mu\text{M}$ ($n = 5$), compared to $0.1 \pm 0.003 \mu\text{M}$ for capsaicin ($n = 5$). 6-Shogaol also appeared to be highly efficacious, with the maximal current response being comparable to the current elicited by a saturating concentration (10 μM) of capsaicin, which activates mTRPV1 channels to an open probability of over 95% (Yang, Xiao, et al., 2015). 6-Gingerol appeared to be a slightly less potent agonist of mTRPV1 channels, with an estimated

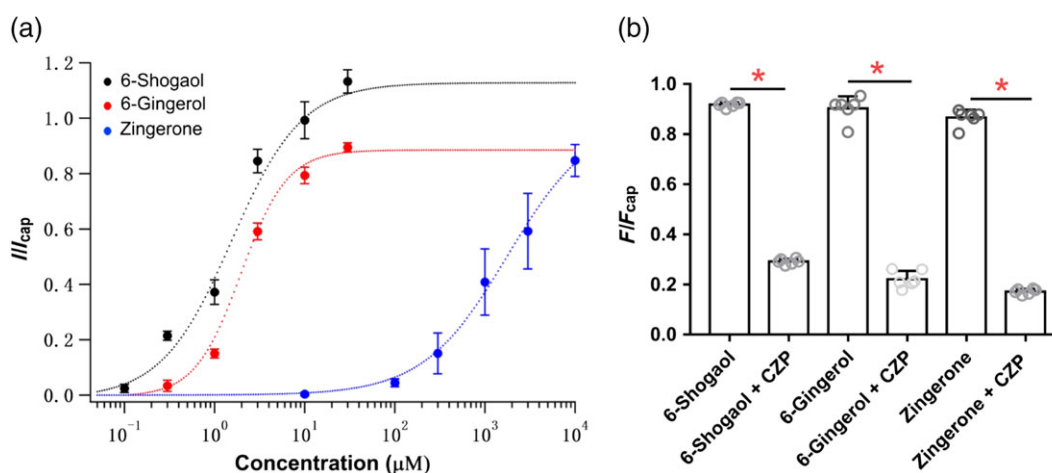


FIGURE 2 Concentration-dependent activation of the wild-type mTRPV1 channels by three ginger compounds. (a) The average current responses to each ginger compound, normalized to that to capsaicin (10 μM), are fitted to a Hill function. $n = 5$. (b) The capsaicin analogue capsazepine (CZP) competitively antagonizes the activation of TRPV1 channels by ginger compounds. Each ginger compound was added alone (10 μM for 6-shogaol and 6-gingerol; 10 mM for zingerone) or together with 10- μM CZP. Calcium imaging responses to capsaicin (10 μM) were used as a positive control for normalization of the fluorescence intensity values. $n = 6$. * $P < .05$, significantly different as indicated; Student's t test

EC₅₀ value $2.9 \pm 0.3 \mu\text{M}$ ($n = 5$) and a maximal response lower than that of saturating concentrations of capsaicin and 6-shogaol (Figure 2a). Zingerone was much less potent, requiring millimolar concentrations of zingerone to elicit an appreciable current. Our results showed that all three pungent ginger compounds were agonists for the mTRPV1 channel, with the order of activation strength being 6-shogaol > 6-gingerol >> zingerone.

3.2 | Ginger compounds bind to the capsaicin binding pocket

To elucidate the structural mechanism, we first tested whether ginger compounds bind to the same ligand-binding pocket in mTRPV1 channels as capsaicin, whose location was clearly identified in cryo-EM electron density maps (Cao et al., 2013; Liao et al., 2013). For this purpose, we tested whether channel activation by ginger compounds could be competitively antagonized by capsazepine, a known capsaicin antagonist that competes for the same ligand-binding site, as verified by cryo-EM structures (Gao, Cao, Julius, & Cheng, 2016). Using live-cell calcium imaging, we confirmed that channel activation by all three ginger compounds could indeed be effectively antagonized by capsazepine (Figure 2b). Previous studies have shown that binding of capsazepine is partly mediated by a hydrogen bond to the T551 residue of TRPV1 channels (Gao et al., 2016). A similar interaction also contributes to the binding of capsaicin, to the carbonyl group in the neck region (Elokely et al., 2016; Yang, Xiao, et al., 2015) that is conserved in the ginger compounds. Our results described below further demonstrated that T551 and another hydrogen bond-forming residue E571 are critical for ginger compounds to activate TRPV1. Based on structural similarities between ginger compounds and capsaicin, we conducted a series of functional tests to investigate specific ligand–host interactions.

3.3 | 6-Shogaol forms the same two hydrogen bonds with mTRPV1 channels as capsaicin

6-Shogaol is structurally similar to capsaicin, with the same functional groups in capsaicin that are known to form hydrogen bonds with T551 and E571 of mTRPV1 channels, and an aliphatic tail that is of a similar length to capsaicin. To test whether 6-shogaol forms the same hydrogen bonds with mTRPV1 channels, we used two mutant channels, T551V and E571A, that would prevent hydrogen bond formation at these sites. Single-channel recordings indicated that 6-shogaol activated both mutants to similar single-channel amplitudes as the WT channel, but that the open probabilities were much lower (Figure 3a). Calcium imaging experiments (Figure 3b) showed that 6-shogaol activated the WT channels with an EC₅₀ value of $0.2 \pm 0.01 \mu\text{M}$ ($n = 6$) (Figure 3C, Table 1). The value is slightly lower than that estimated from current recordings, an observation resembling that for capsaicin (Figure S1). Similar observations were previously reported and attributed to differences in the two detection methods (Geron et al., 2018). Importantly, the T551V mutation shifted the concentration–

response curve substantially to the right, increasing the EC₅₀ value to $3.9 \pm 0.5 \mu\text{M}$ ($n = 6$). The E571A mutation caused an even larger shift, yielding an estimated EC₅₀ value of $451.2 \pm 98.1 \mu\text{M}$ ($n = 6$). The large increases in the EC₅₀ value are consistent with the expectation that 6-shogaol is likely to interact with both T551 and E571 with hydrogen bonding.

Electrophysiological recordings yielded similar results (Figure 3d). Both T551V and E571A substantially reduced the ligand sensitivity of mTRPV1 channels, shifting the concentration–response curve to the right (Figure 3e, Table 2). The E571A mutation again caused a larger shift of the concentration–response curve than T551V. We observed that increasing the 6-shogaol concentration fully compensated for the reduced sensitivity of the T551V mutant. However, increasing the 6-shogaol concentration did not compensate for the reduced sensitivity of the E571A mutant, with the maximal response, estimated from fitting, to be 40% of that to 10- μM capsaicin. These results are comparable to those obtained when capsaicin was used as the agonist for these mutant channels (Yang, Xiao, et al., 2015). Based on these observations, we conclude that 6-shogaol binds to the TRPV1 channel with both the neck-to-T551 and head-to-E571 hydrogen bonds.

3.4 | TRPV1 channel activation by 6-gingerol is also sensitive to mutations at T551 and E571

Compared to 6-shogaol, 6-gingerol contains a hydroxyl group instead of a double bond in the tail (Figure 1b). The additional hydroxyl group reduces the length of the aliphatic chain and can potentially participate in the formation of hydrogen bond like its neighbouring carbonyl group. We found that, at the single-channel level, the open probabilities of the T551V and E571A mutants were substantially lower than that of WT when 10- μM 6-gingerol was used as the agonist (Figure 4a). For WT channels, calcium imaging recordings showed that 6-gingerol was slightly weaker than 6-shogaol in potency, with an estimated EC₅₀ value of $0.3 \pm 0.01 \mu\text{M}$ ($n = 6$) and a maximal response that was 90% of the response to 10- μM capsaicin (Figure 4b,c, Table 1). The T551V and E571A mutations caused at least a one and two orders of magnitude increase in the EC₅₀ value, respectively, highlighting the importance of these hydrogen bond-forming residues for 6-gingerol activation of mTRPV1 channels. Moreover, patch-clamp recordings confirmed that 6-gingerol was slightly less potent than capsaicin and 6-shogaol in activating WT channels and that the T551V and E571A mutations led to dramatic reductions in ligand potency (Figure 4d,e, Table 2). Together, these results confirmed that both T551 and E571 play an important role in mediating interactions between 6-gingerol and mTRPV1 channels.

3.5 | Zingerone is a weak agonist for mTRPV1 channels, yet both T551 and E571 are critical for potency

Zingerone is a shorter version of 6-shogaol, lacking almost all of the aliphatic tail (Figure 1b). Given our observations from 6-shogaol

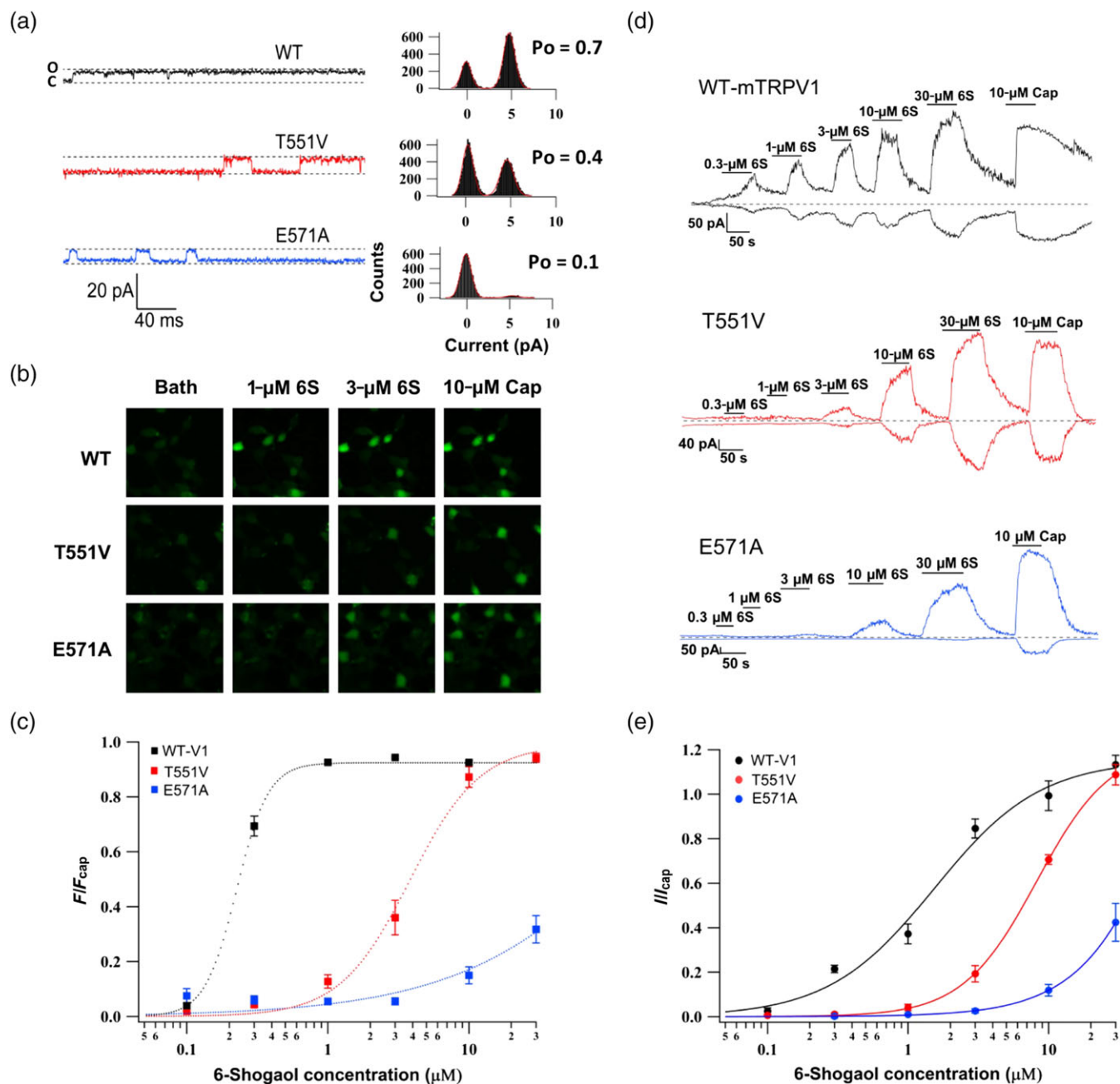


FIGURE 3 6-Shogaol interacts with the TRPV1 channel in a manner similar to that of capsaicin. (a) Representative single-channel current traces recorded in the inside-out configuration at +80 mV in response to 10- μ M 6-shogaol (left) and the corresponding all-point histograms (right) fitted to a double-Gaussian function (red curve). (b) HEK293 cells transiently transfected with wild-type (WT) TRPV1 channels were subjected to calcium imaging before (left) and during (middle) treatment with 6-shogaol, followed by capsaicin treatment (right). (c) Concentration-dependent activation of WT and point mutants by 6-shogaol are fitted to a Hill equation. $n = 6$. (d) Representative current traces from the WT and mutants elicited by applications of 6-shogaol and capsaicin recorded in the inside-out configuration. The holding potential was 0 mV from which testing pulses to +80 mV and -80 mV were applied. (e) The average current responses to 6-shogaol, normalized to that to capsaicin (10 μ M), are fitted to a Hill equation. $n = 5$

described above and previous findings from capsaicin analogues with a progressively shorter tail (Yang, Xiao, et al., 2015), we expected that zingerone would be a weaker agonist than 6-shogaol but its agonist activity was likely to remain dependent on the residues T551 and E571. This turned out to be the case in functional tests. As shown in Figure 5a,b and Table 1, calcium imaging experiments revealed that

zingerone activation of the WT channels occurred at much higher concentrations than that by 6-shogaol and 6-gingerol. Furthermore, the T551V and E571A mutations caused large shifts of the concentration-response curve. In particular, it took more than 0.1-mM zingerone to induce an appreciable response from E571A channels, and the maximal response even at the 30-mM concentration

TABLE 1 Summary of calcium imaging results ($n = 6$ each)

Channel type	Capsaicin		6-Shogaol		6-Gingerol		Zingerone	
	EC ₅₀ (μM)	k	EC ₅₀ (μM)	k	EC ₅₀ (μM)	k	EC ₅₀ (mM)	k
WT	0.1 ± 0.002	1.9	0.2 ± 0.01*	3.8	0.3 ± 0.01* [§]	2.3	0.01 ± 0.001* ^{§,¶}	2.9
T551V	1.0 ± 0.02*	3.3	3.9 ± 0.5 ^{†,}	1.3	4.8 ± 0.4 ^{†,***}	1.5	0.1 ± 0.007 ^{††}	2.1
E571A	1.0 ± 0.04*	3.0	451.2 ± 98.1 ^{†,}	0.6	137.1 ± 18.4 ^{†,***}	0.7	65.6 ± 21.4 ^{††}	0.7

Abbreviations: EC₅₀, effective concentration to achieve 50% of maximal response; k, Hill slope factor; WT, wild type.

* $P < .05$, significantly different from WT channel responding to capsaicin; one-way ANOVA followed by Tukey's post-test.

[†] $P < .05$, significantly different from T551V channel responding to capsaicin; one-way ANOVA followed by Tukey's post-test.

[‡] $P < .05$, significantly different from E571A channel responding to capsaicin; one-way ANOVA followed by Tukey's post-test.

[§] $P < .05$, significantly different from WT channel responding to 6-shogaol; one-way ANOVA followed by Tukey's post-test.

[¶] $P < .05$, significantly different from WT channel responding to 6-gingerol; one-way ANOVA followed by Tukey's post test.

^{||} $P < .05$, significantly different from WT channel responding to 6-shogaol; two-tailed Student t-test.

^{***} $P < .05$, significantly different from WT channel responding to 6-gingerol; two-tailed Student t-test.

^{††} $P < .05$, significantly different from WT channel responding to zingerone; two-tailed Student's t test.

TABLE 2 Summary of electrophysiological measurement results ($n = 5$ each)

Channel type	Capsaicin		6-Shogaol		6-Gingerol		Zingerone	
	EC ₅₀ (μM)	k	EC ₅₀ (μM)	k	EC ₅₀ (μM)	k	EC ₅₀ (mM)	k
WT	0.1 ± 0.003	1.7	1.4 ± 0.1*	1.1	2.9 ± 0.3* [§]	1.7	2.6 ± 0.9* ^{§,¶}	0.9
T551V	1.4 ± 0.03*	1.8	8.1 ± 0.5	1.5	32.7 ± 3.1 ^{†,***}	1.5	15.2 ± 5.0 ^{††}	1.2
E571A	1.3 ± 0.03*	1.8	27.1 ± 5.0 ^{†,}	1.7	109.7 ± 37.4 ^{†,***}	0.7	165.9 ± 61.2 ^{††}	1.0

Abbreviations: EC₅₀, effective concentration to achieve 50% of maximal response; k, Hill slope factor; WT, wild type.

* $P < .05$, significantly different from WT channel responding to capsaicin, one-way ANOVA followed by Tukey's post test.

[†] $P < .05$, significantly different from T551V channel responding to capsaicin, one-way ANOVA followed by Tukey's post-test

[‡] $P < .05$, significantly different from E571A channel responding to capsaicin, one-way ANOVA followed by Tukey's post test.

[§] $P < .05$, significantly different from WT channel responding to 6-shogaol, one-way ANOVA followed by Tukey's post test.

[¶] $P < .05$, significantly different from WT channel responding to 6-gingerol, one-way ANOVA followed by Tukey's post test.

^{||} $P < .05$, significantly different from WT channel responding to 6-shogaol, two-tailed Student's t test.

^{***} $P < .05$, significantly different from WT channel responding to 6-gingerol, two-tailed Student's t test.

^{††} $P < .05$, significantly different from WT channel responding to zingerone, two-tailed Student's t test.

was much lower than the level that could be reached in the WT and T551V channels. All these findings from calcium imaging were satisfactorily confirmed by patch-clamp recordings (Figure 5c,d, Table 2).

In summary, functional tests suggested that the ginger spicy compounds bind to the TRPV1 channel at the same binding pocket, with their potencies depending on both the aliphatic tail of the agonists and the hydrogen bond-forming residues of the channel.

3.6 | Structural modelling of atomic interactions between ginger compounds and TRPV1 channels

We assessed atom-specific interactions between ginger compounds and the TRPV1 channel by computational structural modelling. Using an updated version of RosettaLigand application (Bender et al., 2016;

Davis et al., 2009; Davis & Baker, 2009; Meiler & Baker, 2006), we first examined the interactions between 6-shogaol and the TRPV1 channel. Energy minimization procedure yielded two groups of binding poses that were only slightly different (Figure 6a,b, top panels; Figure S2). Both poses resemble that of capsaicin in that the 6-shogaol molecule adopted a "head-down tail-up" orientation stabilized partially by two hydrogen bonds with T551 and E571, an observation corroborating results from our functional tests of mutant channels (Figure 3). Binding energy distributions of hydrogen bonds and VDW interactions were also similar to those of capsaicin (Figure 6c, top panel). A major difference, however, was that the 6-shogaol tail took a relatively stable position, whereas the capsaicin tail alternated among multiple positions (Yang, Xiao, et al., 2015). The preferable position of the 6-shogaol tail appeared to be due to the C=C bond at its base, which restricts the tail's rotational freedom. In comparison, capsaicin has a single C=C bond located near the tip

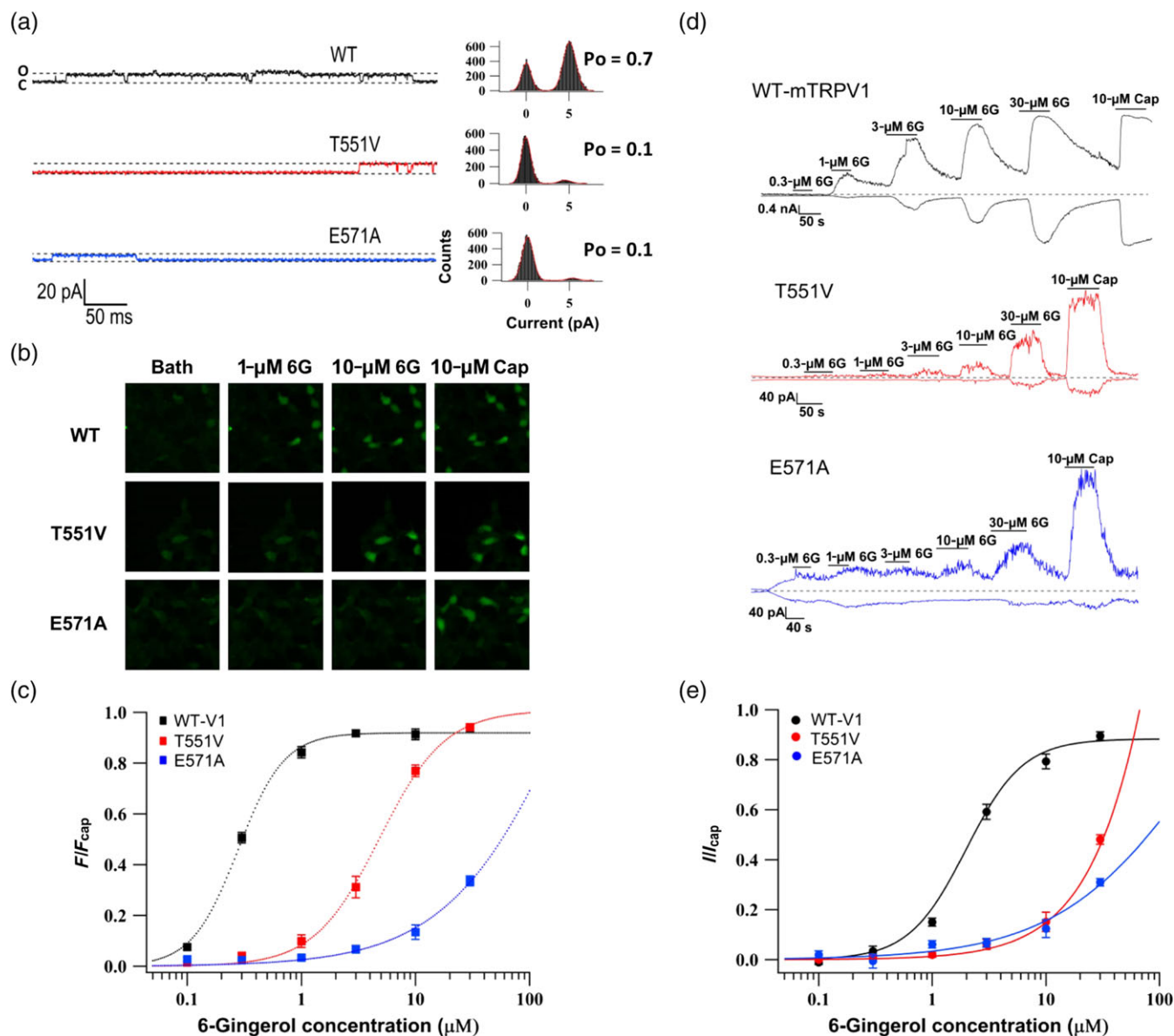


FIGURE 4 Residues T551 and E571 are critical for activation of the TRPV1 channel by 6-gingerol. (a) Representative single-channel current traces recorded in the inside-out configuration at +80 mV in response to 10- μ M 6-gingerol (left) and the corresponding all-point histograms (right) fitted to a double-Gaussian function (red curve). (b) HEK293 cells transiently transfected with wild-type (WT) TRPV1 channels were subjected to calcium imaging before (left) and during (middle) treatment with 6-gingerol, followed by capsaicin treatment (right). (c) Concentration-dependent activation of WT and point mutants by 6-gingerol are fitted to a Hill equation. $n = 6$. (d) Representative current traces from the WT and mutants elicited by applications of 6-gingerol and capsaicin recorded in the inside-out configuration. (e) The average current responses to 6-gingerol, normalized to that to capsaicin (10 μ M), are fitted to a Hill equation. $n = 5$

of its tail. Indeed, flapping of the capsaicin tail was seen mostly at its base (Yang, Xiao, et al., 2015). Our structural modelling results are consistent with functional data, suggesting that 6-shogaol activates TRPV1 channels in a manner very similar to that of capsaicin.

Structural modelling of 6-gingerol revealed many similarities to 6-shogaol but also noticeable differences. As shown in Figure 6a,b, middle panels, and Figure S1, many of the top 30 poses were similar to those of capsaicin and 6-shogaol in orientation and participation of T551 and E571 in the formation of hydrogen bonds. In particular, the neck-to-T551 hydrogen bond was frequently observed, and the head-to-E571 hydrogen bond was also observed. These observations

are consistent with our functional data showing that replacing T551 and E571 with a hydrophobic residue substantially reduced 6-gingerol's potency (Figure 4). Interestingly, the gingerol head was seen in some models to be in close proximity to Y512, a key residue for capsaicin activation (Jordt & Julius, 2002; Yang, Xiao, et al., 2015). Another noticeable observation from the modelling results was that the bound 6-gingerol appeared to be less stable and not converging on specific binding poses among the top 30 models (Figure 6a,b, middle; Figure S2). These results are again consistent with functional data exhibiting that 6-gingerol is a weaker agonist than capsaicin (Figures 2a and 4).

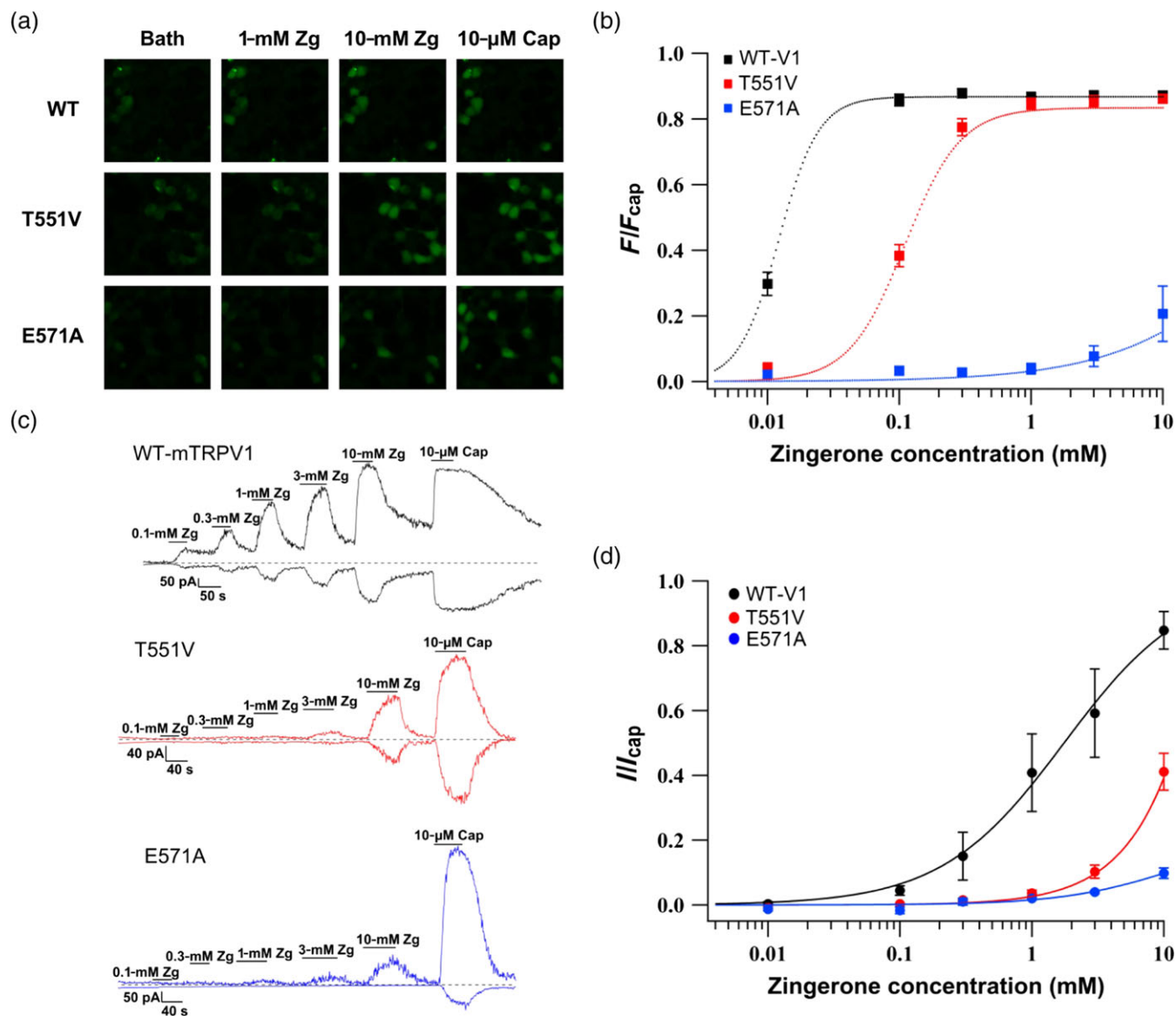


FIGURE 5 Mechanism for zingerone-induced TRPV1 channel activation. (a) HEK293 cells transiently transfected with wild-type TRPV1 channels were subjected to calcium imaging before (left) and during (middle) treatment with zingerone, followed by capsaicin treatment (right). (b) Concentration-dependent activation of WT and point mutants by zingerone are fitted to a Hill equation. $n = 6$. (c) Representative current traces from the WT and mutants elicited by applications of zingerone and capsaicin recorded in the inside-out configuration. (d) The average current responses to zingerone, normalized to that to capsaicin (10 μ M), are fitted to a Hill equation. $n = 5$

Predicting zingerone binding by structural modelling was more challenging (Figure 6, bottom panels; Figure S2), as expected for this weak agonist. Many of the top 30 models had zingerone bound in a similar pose as capsaicin; for example, 17 of them indicated a possible hydrogen bond between the zingerone neck and T551, whereas seven of them indicated a possible hydrogen bond between the zingerone head and E571. This is again consistent with functional data from mutant channels. However, many other ligand-binding poses were seen among the top models. One factor contributing to these new binding poses was the substantial reduction of VDW interactions due to the shortened tail that contributes to the stabilization of both the orientation and binding affinity of capsaicin, 6-shogaol, and 6-

gingerol. Interestingly, five of the top models had the hydroxyl group on the zingerone head in close proximity to T671 in the S6 segment, indicating the possibility of forming a hydrogen bond. Indeed, the average Rosetta energy for hydrogen bond of the top models was substantial at this position (Figure 6c, bottom panel). This interaction, if formed, would contribute to the stabilization of ligand binding and, given the role played by the S6 segment in activation of the TRPV1 channel (Yang et al., 2018; Zheng & Ma, 2014), may even represent a new way to stabilize the channel's open conformation. Overall, our structural modelling results confirmed that zingerone is much less stable inside the ligand-binding pocket and, as a result, a weak agonist for the TRPV1 channel.

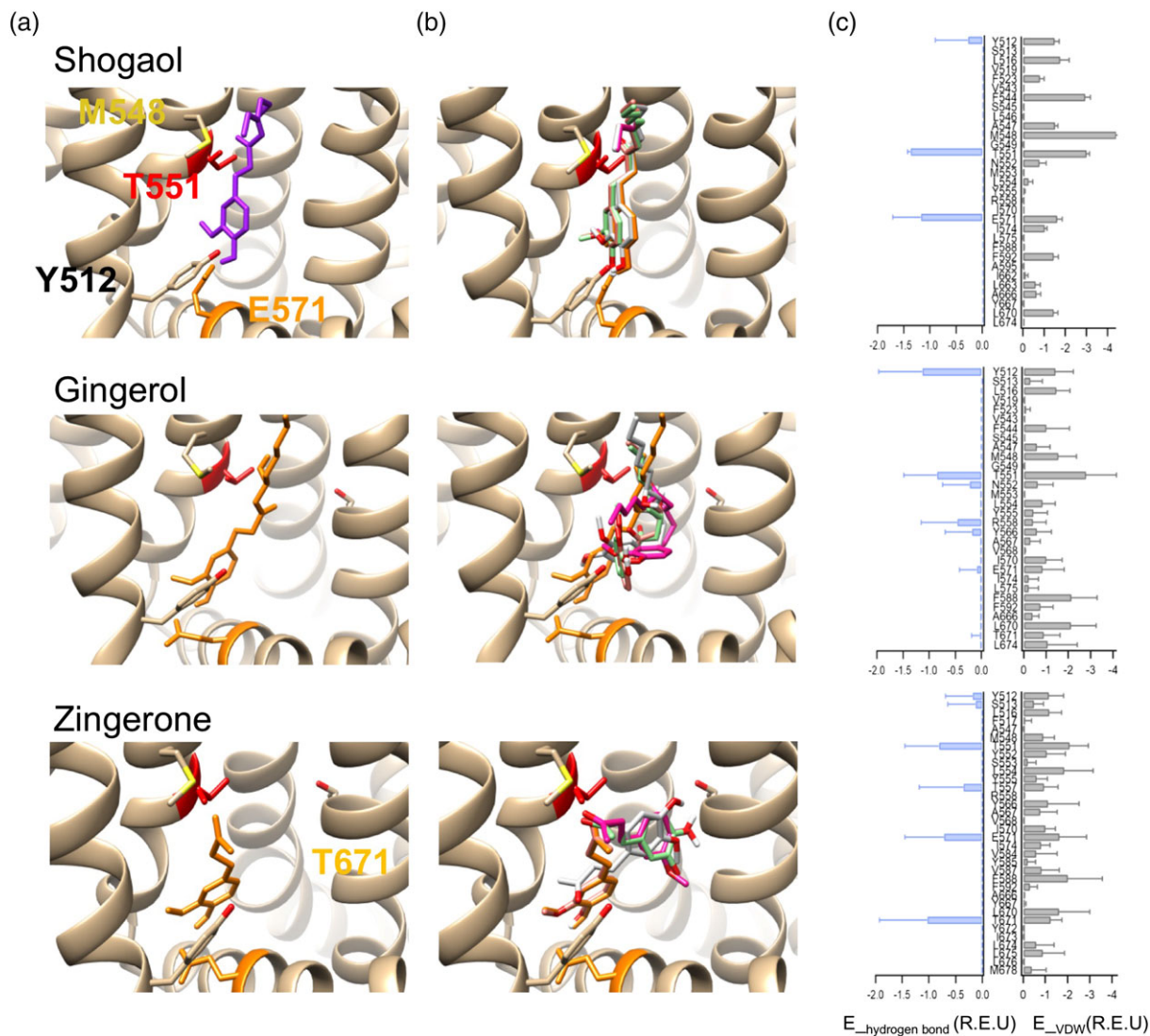


FIGURE 6 Molecular modelling of interactions between ginger compounds and the TRPV1 channel. (a) Representative binding pose observed within the 0.1% lowest energy models (compounds in orange). (b) Additional examples of top binding poses. (c) Hydrogen bond and VDW interaction energies mapped on a per residue basis (0.1% lowest energy models) between the channel and respective vanilloid compound. Unit of energy is Rosetta Energy Unit (R.E.U.)

3.7 | Functional confirmation of zingerone interaction with T671 on S6

The computational modelling results predicted that zingerone could potentially interact with T671 on the S6 segment (Figure 7a). In order to test this intriguing prediction, we conducted functional tests on a conserved mutation, T671S, at this critical position for gating. Patch-clamp recordings demonstrated that this subtle structural perturbation indeed could produce substantial effects on zingerone activation. The T671S mutant channels yielded very small currents to 10-mM zingerone, although their responses to capsaicin remained robust (Figure 7b) as reported previously (Yang, Xiao, et al., 2015). As a result, the estimated EC₅₀ value for zingerone activation of T671S was 141.6 ± 46.6 mM ($n = 5$), which was significantly higher than the EC₅₀ value of the WT channels (2.6 ± 0.9 mM, $n = 5$; Figure 7c,d). These observations are consistent with the existence of a direct

interaction between zingerone (but not capsaicin) and T671 on S6, suggesting that this tail-less ginger compound might take two alternative binding poses—a vertical pose used by capsaicin and other ginger compounds and a novel horizontal pose in which it forms a bridge between S4 and S6.

4 | DISCUSSION

In the present study, we analysed interactions between ginger compounds and the TRPV1 channel, focusing on potential key contacts they make in the binding pocket. The general picture emerging from this study suggested a clear resemblance between ginger compounds and bound capsaicin, including the “head-down tail-up” orientation and the two key hydrogen bonds, as well as a potentially new way for zingerone to interact with the channel. The comparative analysis

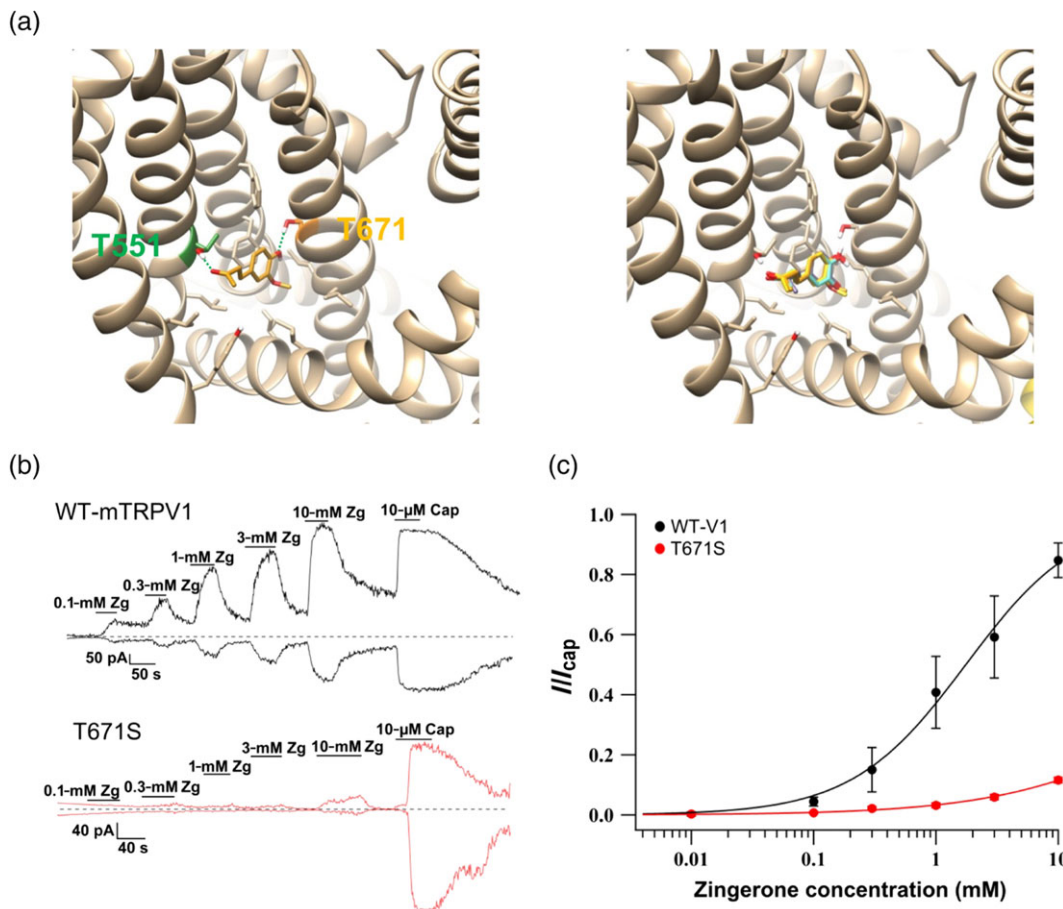


FIGURE 7 Zingerone directly interacts with T671 in S6. (a) Representative horizontal poses of zingerone in which a direct interaction with T671 is observed. (b) Representative current traces from wild-type (WT) and T671S mutant channels treated with zingerone. (c) The average current responses of WT channels and T671S to zingerone, normalized to that to capsaicin (10 μ M), are fitted to a Hill equation. $n = 5$

among the three ginger compounds, together with capsaicin, revealed a number of important structural details relating to their different potencies, which will be discussed below.

Among the three tested ginger compounds, 6-shogaol is the most similar to capsaicin in molecular structure. Hence, functional differences between the two can be reliably associated to their distinct structural features. There are three structural elements in 6-shogaol that are different from capsaicin: the absence of the neck amide, a different location of the C=C bond, and a shorter aliphatic tail, by two carbons. The replacement of the neck amide in capsaicin with an ester (yielding capsate) produced a two order of magnitude shift in the concentration–response relationship (Yang, Xiao, et al., 2015). In contrast, the difference between 6-shogaol and capsaicin is less. Together with the very similar binding poses between 6-shogaol and capsaicin predicted by computational modelling, these observations suggest that the structural difference in the neck region of 6-shogaol might have a minor effect on the hydrogen bonding strength of the neighbouring carbonyl, or/and there might be a compensatory effect from the C=C double bond on the other side of the carbonyl. The presence of a C=C bond in the capsaicin tail, by itself, has long been recognized as unlikely to be important for pungency, as removing it yielded a compound of similar spiciness to capsaicin (Nelson &

Dawson, 1923), and that the aliphatic tail can take multiple positions in the bonding pocket with apparently compatible binding energies (Yang, Xiao, et al., 2015). Shifting the C=C bond to the base of the shogaol tail limits the rotational freedom in this region, restricting the shogaol tail to only one of the multiple possible positions, as seen in our computational models. Indeed, removing the C=C bond from 6-shogaol yields paradol, a pungent compound found in *Melegueta* peppers (a.k.a. grains of paradise) from West Africa (Riera et al., 2009). The shorter tail in 6-shogaol, however, may be more than sufficient to explain its slightly lower potency, because shortening the capsaicin tail has a major impact on potency (Yang, Xiao, et al., 2015). A similar conclusion can be drawn from 6-gingerol and zingerone (see below).

In comparison to 6-shogaol, 6-gingerol contains a hydroxyl group in place of the C=C bond. This structural alternation has two consequences: introduction of an alternative hydrogen bond forming group adjacent to the neck carbonyl and shortening of the aliphatic tail. Indeed, we observed that the hydroxyl group may replace the neck carbonyl in interacting with T551 (Figure 6a,b, middle). A possible polar interaction between this hydroxyl group and T671 on the pore-forming S6 segment was also occasionally observed. The hydroxyl group in gingerol effectively shortens its aliphatic tail, reducing VDW interactions within the hydrophobic pocket of the ligand-binding

domain. This effect is likely to be a major factor for the lower potency of 6-gingerol in comparison to 6-shogaol and capsaicin. Consistent with this expectation, adding a hydroxyl group to the capsaicin tail yields capsaicinol, a much less potent compound (Kobata et al., 2006). The hydroxyl group not only shortens the aliphatic tail but also forces the bound 6-gingerol to shift downwards in comparison to capsaicin due to its tendency to reside in the more hydrophilic lower part of the binding pocket—both changes reduce the opportunities for VDW interactions known to contribute substantially to capsaicin binding (Yang, Xiao, et al., 2015). In support of this view, 8-gingerol and 10-gingerol, having progressively longer tails, are found to be more potent than 6-gingerol in activating TRPV1 channels (Morita, Iwasaki, Kobata, Yokogoshi, & Watanabe, 2007), whereas shortening the gingerol tail has a detrimental effect (Dedov et al., 2002).

Zingerone is a shortened version of 6-shogaol, lacking most of its tail. As discussed above, the aliphatic tail contributes substantially to VDW interactions. It is therefore not surprising that the absence of an aliphatic tail in zingerone results in a much lower potency. Our molecular modelling and functional results confirmed this expectation. Interestingly, in the absence of a real tail and its associated hydrophobic interactions with the upper part of the ligand-binding pocket, the “head-down tail-up” orientation of zingerone becomes unstable, an observation highlighting the anchoring role of the aliphatic tail in ligand binding. We observed that zingerone can potentially find an alternative pose inside the binding domain, where it interacts with T671 of S6. This new interaction, not seen between capsaicin and TRPV1, allows zingerone to directly bridge S4 (probably an immobile channel structure according to cryo-EM data of multiple TRPV1 channel states; Cao et al., 2013; Gao et al., 2016; Liao et al., 2013) and S6. The horizontal pose of zingerone represents a new way to influence the channel pore. The combination of the effects discussed above is likely to contribute to the much lower potency of zingerone. Indeed, it has been suggested that, due to its poor potency for TRPV1 channels, zingerone may instead interact with TRPA1 channels when tested on the rat spinal cord slices (Yue, Jiang, Fujita, & Kumamoto, 2013).

In summary, our data suggest that the three ginger pungent compounds, which share the same vanillyl head group, interact with the S4-S5 linker of the TRPV1 channel in the same manner as capsaicin. They also appear to form the same hydrogen bond interaction with S4 that attaches capsaicin to the ligand-binding domain. Minor structural deviations in the neck region do not seem to substantially alter the interaction with the TRPV1 channel or its energetics. The length of the aliphatic tail, the position of the C=C bond, and the additional hydroxyl group all play a role in determining the orientation, contacts, and stability of the ligand-channel interaction, resulting in great variations in ligand-induced channel activity. These findings offer a structural explanation why ginger aging (which converts gingerol to shogaol) enhances the perceived spiciness, whereas cooking gingers (which converts gingerol and shogaol to zingerone) substantially reduces their spiciness. Information from this study should be useful for guiding pharmaceutical efforts searching for non-addictive analgesics, targeting the nociceptive TRPV1 ion channel.

ACKNOWLEDGEMENTS

We thank Dr. Kewei Wang and our current and former lab members for their generous help and insightful discussion. This work is supported by funding from the Qingdao Postdoctoral Research Project to YHT and National Institute of Neurological Disorders and Stroke (R01NS103954) to J.Z. and V.Y.Y.

CONFLICT OF INTEREST

The authors declare no conflicts of interest.

AUTHOR CONTRIBUTIONS

Y.Y., Y.D., S.V., and F.Y. performed the experiments, J.Z. designed the study and wrote the manuscript with Y.Y. and Y.T., Y.T. and J.Z. supervised the study, and all authors participated in data analysis and manuscript editing and approved the manuscript.

DECLARATION OF TRANSPARENCY AND SCIENTIFIC RIGOUR

This Declaration acknowledges that this paper adheres to the principles for transparent reporting and scientific rigour of preclinical research as stated in the *BJP* guidelines for [Design & Analysis](#), and as recommended by funding agencies, publishers and other organisations engaged with supporting research.

ORCID

Yuhua Tian  <https://orcid.org/0000-0001-8239-6560>

Jie Zheng  <https://orcid.org/0000-0002-4161-627X>

REFERENCES

- Alexander, S. P., Striessnig, J., Kelly, E., Marrion, N. V., Peters, J. A., Faccenda, E., ... CGTP Collaborators (2017). The concise guide to pharmacology 2017/18: Voltage-gated ion channels. *British Journal of Pharmacology*, 174(Suppl 1), S160–S194. <https://doi.org/10.1111/bph.13884>
- Aslani, A., Ghannadi, A., & Rostami, F. (2016). Design, formulation, and evaluation of ginger medicated chewing gum. *Adv Biomed Res*, 5, 130. <https://doi.org/10.4103/2277-9175.187011>
- Barth, P., Schonbrun, J., & Baker, D. (2007). Toward high-resolution prediction and design of transmembrane helical protein structures. *Proceedings of the National Academy of Sciences of the United States of America*, 104(40), 15682–15687. <https://doi.org/10.1073/pnas.0702515104>
- Bender, B. J., Cisneros, A. 3rd, Duran, A. M., Finn, J. A., Fu, D., Lokits, A. D., ... Moretti, R. (2016). Protocols for molecular modeling with Rosetta3 and RosettaScripts. *Biochemistry*, 55(34), 4748–4763. <https://doi.org/10.1021/acs.biochem.6b00444>
- Cao, E., Liao, M., Cheng, Y., & Julius, D. (2013). TRPV1 structures in distinct conformations reveal activation mechanisms. *Nature*, 504(7478), 113–118. <https://doi.org/10.1038/nature12823>
- Caterina, M. J., Schumacher, M. A., Tominaga, M., Rosen, T. A., Levine, J. D., & Julius, D. (1997). The capsaicin receptor: A heat-activated ion channel in the pain pathway. *Nature*, 389(6653), 816–824. <https://doi.org/10.1038/39807>
- Cheng, W., Yang, F., Takanishi, C. L., & Zheng, J. (2007). Thermosensitive TRPV channel subunits coassemble into heteromeric channels with

- intermediate conductance and gating properties. *Journal of General Physiology*, 129(3), 191–207. <https://doi.org/10.1085/jgp.200709731>
- Chrubasik, S., Pittler, M. H., & Roufogalis, B. D. (2005). Zingiberis rhizoma: A comprehensive review on the ginger effect and efficacy profiles. *Phytomedicine*, 12(9), 684–701. <https://doi.org/10.1016/j.phymed.2004.07.009>
- Curtis, M. J., Alexander, S., Cirino, G., Docherty, J. R., George, C. H., Giembycz, M. A., ... Ahluwalia, A. (2018). Experimental design and analysis and their reporting II: Updated and simplified guidance for authors and peer reviewers. *British Journal of Pharmacology*, 175(7), 987–993. <https://doi.org/10.1111/bph.14153>
- Darre, L., & Domene, C. (2015). Binding of capsaicin to the TRPV1 ion channel. *Molecular Pharmaceutics*, 12(12), 4454–4465. <https://doi.org/10.1021/acs.molpharmaceut.5b00641>
- Davis, I. W., & Baker, D. (2009). RosettaLigand docking with full ligand and receptor flexibility. *Journal of Molecular Biology*, 385(2), 381–392. <https://doi.org/10.1016/j.jmb.2008.11.010>
- Davis, I. W., Raha, K., Head, M. S., & Baker, D. (2009). Blind docking of pharmaceutically relevant compounds using RosettaLigand. *Protein Science*, 18(9), 1998–2002. <https://doi.org/10.1002/pro.192>
- Dedov, V. N., Tran, V. H., Duke, C. C., Connor, M., Christie, M. J., Mandadi, S., & Roufogalis, B. D. (2002). Gingerols: A novel class of vanilloid receptor (VR1) agonists. *British Journal of Pharmacology*, 137(6), 793–798. <https://doi.org/10.1038/sj.bjp.0704925>
- Elokely, K., Velisetty, P., Delemotte, L., Palovcak, E., Klein, M. L., Rohacs, T., & Carnevale, V. (2016). Understanding TRPV1 activation by ligands: Insights from the binding modes of capsaicin and resiniferatoxin. *Proceedings of the National Academy of Sciences of the United States of America*, 113(2), E137–E145. <https://doi.org/10.1073/pnas.1517288113>
- Gao, Y., Cao, E., Julius, D., & Cheng, Y. (2016). TRPV1 structures in nanodiscs reveal mechanisms of ligand and lipid action. *Nature*, 534(7607), 347–351. <https://doi.org/10.1038/nature17964>
- Geron, M., Kumar, R., Zhou, W., Faraldo-Gomez, J. D., Vasquez, V., & Priel, A. (2018). TRPV1 pore turret dictates distinct DkTx and capsaicin gating. *Proceedings of the National Academy of Sciences of the United States of America*, 115(50), E11837–e11846. <https://doi.org/10.1073/pnas.1809662115>
- Govindarajan, V. S. (1982a). Ginger—Chemistry, technology, and quality evaluation: Part 1. *Critical Reviews in Food Science and Nutrition*, 17(1), 1–96. <https://doi.org/10.1080/10408398209527343>
- Govindarajan, V. S. (1982b). Ginger—Chemistry, technology, and quality evaluation: Part 2. *Critical Reviews in Food Science and Nutrition*, 17(3), 189–258. <https://doi.org/10.1080/10408398209527348>
- Grant, K. L., & Lutz, R. B. (2000). Ginger. *American Journal of Health-System Pharmacy*, 57(10), 945–947. <https://doi.org/10.1093/ajhp/57.10.945>
- Han, Y., Li, B., Yin, T. T., Xu, C., Ombati, R., Luo, L., ... Lai, R. (2018). Molecular mechanism of the tree shrew's insensitivity to spiciness. *PLoS Biology*, 16(7), e2004921. <https://doi.org/10.1371/journal.pbio.2004921>
- Harding, S. D., Sharman, J. L., Faccenda, E., Southan, C., Pawson, A. J., Ireland, S., ... NC-IUPHAR (2018). The IUPHAR/BPS guide to pharmacology in 2018: Updates and expansion to encompass the new guide to immunopharmacology. *Nucleic Acids Research*, 46(D1), D1091–d1106. <https://doi.org/10.1093/nar/gkx1121>
- Hawkins, P. C., & Nicholls, A. (2012). Conformer generation with OMEGA: Learning from the data set and the analysis of failures. *Journal of Chemical Information and Modeling*, 52(11), 2919–2936. <https://doi.org/10.1021/ci300314k>
- Hawkins, P. C., Skillman, A. G., Warren, G. L., Ellingson, B. A., & Stahl, M. T. (2010). Conformer generation with OMEGA: Algorithm and validation using high quality structures from the Protein Databank and Cambridge Structural Database. *Journal of Chemical Information and Modeling*, 50(4), 572–584. <https://doi.org/10.1021/ci100031x>
- Iwasaki, Y., Morita, A., Iwasawa, T., Kobata, K., Sekiwa, Y., Morimitsu, Y., ... Watanabe, T. (2006). A nonpungent component of steamed ginger—[10]-shogaol—increases adrenaline secretion via the activation of TRPV1. *Nutritional Neuroscience*, 9(3–4), 169–178. <https://doi.org/10.1080/10284150600955164>
- Jordt, S. E., & Julius, D. (2002). Molecular basis for species-specific sensitivity to “hot” chili peppers. *Cell*, 108(3), 421–430. [https://doi.org/10.1016/S0092-8674\(02\)00637-2](https://doi.org/10.1016/S0092-8674(02)00637-2)
- Kobata, K., Iwasawa, T., Iwasaki, Y., Morita, A., Suzuki, Y., Kikuzaki, H., ... Watanabe, T. (2006). Capsaicinol: Synthesis by allylic oxidation and its effect on TRPV1-expressing cells and adrenaline secretion in rats. *Bioscience, Biotechnology, and Biochemistry*, 70(8), 1904–1912. <https://doi.org/10.1271/bbb.60064>
- Kumar, R., Hazan, A., Basu, A., Zalzman, N., Matzner, H., & Priel, A. (2016). Tyrosine residue in the TRPV1 vanilloid binding pocket regulates deactivation kinetics. *Journal of Biological Chemistry*, 291(26), 13855–13863. <https://doi.org/10.1074/jbc.M116.726372>
- Lemmon, G., & Meiler, J. (2012). Rosetta ligand docking with flexible XML protocols. *Methods in Molecular Biology*, 819, 143–155. https://doi.org/10.1007/978-1-61779-465-0_10
- Liao, M., Cao, E., Julius, D., & Cheng, Y. (2013). Structure of the TRPV1 ion channel determined by electron cryo-microscopy. *Nature*, 504(7478), 107–112. <https://doi.org/10.1038/nature12822>
- Lien, H. C., Sun, W. M., Chen, Y. H., Kim, H., Hasler, W., & Owyang, C. (2003). Effects of ginger on motion sickness and gastric slow-wave dysrhythmias induced by circularvection. *American Journal of Physiology. Gastrointestinal and Liver Physiology*, 284(3), G481–G489. <https://doi.org/10.1152/ajpgi.00164.2002>
- Meiler, J., & Baker, D. (2006). ROSETTALIGAND: Protein-small molecule docking with full side-chain flexibility. *Proteins*, 65(3), 538–548. <https://doi.org/10.1002/prot.21086>
- Morita, A., Iwasaki, Y., Kobata, K., Yokogoshi, H., & Watanabe, T. (2007). Newly synthesized oleylgingerol and oleylshogaol activate TRPV1 ion channels. *Bioscience, Biotechnology, and Biochemistry*, 71(9), 2304–2307. <https://doi.org/10.1271/bbb.70187>
- Nelson, E. K., & Dawson, L. E. (1923). The constitution of capsaicin, the pungent principle of capsium. III. *Journal of the American Chemical Society*, 45, 2179–2181. <https://doi.org/10.1021/ja01662a023>
- Ohbuchi, K., Mori, Y., Ogawa, K., Warabi, E., Yamamoto, M., & Hirokawa, T. (2016). Detailed analysis of the binding mode of vanilloids to transient receptor potential vanilloid type I (TRPV1) by a mutational and computational study. *PLoS ONE*, 11(9), e0162543. <https://doi.org/10.1371/journal.pone.0162543>
- Parry, J. W. (1969). *Spices* (Vol. 2). New York: Chemical Publishing Co Inc.
- Pettersen, E. F., Goddard, T. D., Huang, C. C., Couch, G. S., Greenblatt, D. M., Meng, E. C., & Ferrin, T. E. (2004). UCSF Chimera—A visualization system for exploratory research and analysis. *Journal of Computational Chemistry*, 25(13), 1605–1612. <https://doi.org/10.1002/jcc.20084>
- Riera, C. E., Menozzi-Smarrito, C., Affolter, M., Michlig, S., Munari, C., Robert, F., ... le Coutre, J. (2009). Compounds from Sichuan and Melegueta peppers activate, covalently and non-covalently, TRPA1 and TRPV1 channels. *British Journal of Pharmacology*, 157(8), 1398–1409. <https://doi.org/10.1111/j.1476-5381.2009.00307.x>
- Siemens, J., Zhou, S., Piskrowski, R., Nikai, T., Lumpkin, E. A., Basbaum, A. I., ... Julius, D. (2006). Spider toxins activate the capsaicin receptor to produce inflammatory pain. *Nature*, 444(7116), 208–212. <https://doi.org/10.1038/nature05285>

- Tominaga, M., Caterina, M. J., Malmberg, A. B., Rosen, T. A., Gilbert, H., Skinner, K., ... Julius, D. (1998). The cloned capsaicin receptor integrates multiple pain-producing stimuli. *Neuron*, 21(3), 531–543. [https://doi.org/10.1016/S0896-6273\(00\)80564-4](https://doi.org/10.1016/S0896-6273(00)80564-4)
- Yang, F., Vu, S., Yarov-Yarovoy, V., & Zheng, J. (2016). Rational design and validation of a vanilloid-sensitive TRPV2 ion channel. *Proceedings of the National Academy of Sciences of the United States of America*, 113(26), E3657–E3666. <https://doi.org/10.1073/pnas.1604180113>
- Yang, F., Xiao, X., Cheng, W., Yang, W., Yu, P., Song, Z., ... Zheng, J. (2015). Structural mechanism underlying capsaicin binding and activation of the TRPV1 ion channel. *Nature Chemical Biology*, 11(7), 518–524. <https://doi.org/10.1038/nchembio.1835>
- Yang, F., Xiao, X., Lee, B. H., Vu, S., Yang, W., Yarov-Yarovoy, V., & Zheng, J. (2018). The conformational wave in capsaicin activation of transient receptor potential vanilloid 1 ion channel. *Nature Communications*, 9(1), 2879. <https://doi.org/10.1038/s41467-018-05339-6>
- Yang, F., & Zheng, J. (2017). Understand spiciness: Mechanism of TRPV1 channel activation by capsaicin. *Protein & Cell*, 8(3), 169–177. <https://doi.org/10.1007/s13238-016-0353-7>
- Yang, S. L., Yang, F., Wei, N. N., Hong, J., Li, B. W., Luo, L., ... Lai, R. (2015). A pain-inducing centipede toxin targets the heat activation machinery of nociceptor TRPV1. *Nature Communications*, 6, 8297. <https://doi.org/10.1038/ncomms9297>
- Yarov-Yarovoy, V., Baker, D., & Catterall, W. A. (2006). Voltage sensor conformations in the open and closed states in ROSETTA structural models of K(+) channels. *Proceedings of the National Academy of Sciences of the United States of America*, 103(19), 7292–7297. <https://doi.org/10.1073/pnas.0602350103>
- Yarov-Yarovoy, V., DeCaen, P. G., Westenbroek, R. E., Pan, C. Y., Scheuer, T., Baker, D., & Catterall, W. A. (2012). Structural basis for gating charge movement in the voltage sensor of a sodium channel. *Proceedings of the National Academy of Sciences of the United States of America*, 109(2), E93–E102. <https://doi.org/10.1073/pnas.1118434109>
- Yarov-Yarovoy, V., Schonbrun, J., & Baker, D. (2006). Multipass membrane protein structure prediction using Rosetta. *Proteins*, 62(4), 1010–1025. <https://doi.org/10.1002/prot.20817>
- Yue, H. Y., Jiang, C. Y., Fujita, T., & Kumamoto, E. (2013). Zingerone enhances glutamatergic spontaneous excitatory transmission by activating TRPA1 but not TRPV1 channels in the adult rat substantia gelatinosa. *Journal of Neurophysiology*, 110(3), 658–671. <https://doi.org/10.1152/jn.00754.2012>
- Zhang, F., Hanson, S. M., Jara-Oseguera, A., Krepiy, D., Bae, C., Pearce, L. V., ... Swartz, K. J. (2016). Engineering vanilloid-sensitivity into the rat TRPV2 channel. *eLife*, 5. <https://doi.org/10.7554/eLife.16409>
- Zheng, J. (2013). Molecular mechanism of TRP channels. *Comprehensive Physiology*, 3(1), 221–242. <https://doi.org/10.1002/cphy.c120001>
- Zheng, J., & Ma, L. (2014). Structure and function of the thermoTRP channel pore. *Current Topics in Membranes*, 74, 233–257. <https://doi.org/10.1016/b978-0-12-800181-3.00009-9>

SUPPORTING INFORMATION

Additional supporting information may be found online in the Supporting Information section at the end of the article.

How to cite this article: Yin Y, Dong Y, Vu S, et al. Structural mechanisms underlying activation of TRPV1 channels by pungent compounds in gingers. *Br J Pharmacol*. 2019;176:3364–3377. <https://doi.org/10.1111/bph.14766>